Searching for new white dwarf pulsators for TESS observations at Konkoly Observatory

Zs Bognár, Cs Kalup, Á. Sódor, S. Charpinet, J. J. Hermes

Searching for new white dwarf pulsators for *TESS* observations at Konkoly Observatory

Zs. Bognár,[1]★ Cs. Kalup,[1,2] Á. Sódor,[1] S. Charpinet[3,4] and J. J. Hermes[5]†

[1]*Konkoly Observatory, MTA Research Centre for Astronomy and Earth Sciences, Konkoly Thege Miklós út 15-17, H–1121 Budapest*
[2]*Eötvös University, Department of Astronomy, Pf. 32, 1518, Budapest, Hungary*
[3]*Université de Toulouse, UPS-OMP, IRAP, Toulouse, F-31400, France*
[4]*CNRS, IRAP, 14 avenue Edouard Belin, F-31400 Toulouse, France*
[5]*Department of Physics and Astronomy, University of North Carolina, Chapel Hill, NC – 27599-3255, USA*

ABSTRACT

We present the results of our survey searching for new white dwarf pulsators for observations by the *TESS* space telescope. We collected photometric time-series data on 14 white dwarf variable candidates at Konkoly Observatory, and found two new bright ZZ Ceti stars, namely EGGR 120 and WD 1310+583. We performed a Fourier analysis of the datasets. In the case of EGGR 120, which was observed on one night only, we found one significant frequency at 1332 µHz with 2.3 mmag amplitude. We successfully observed WD 1310+583 on eight nights, and determined 17 significant frequencies in the whole dataset. Seven of them seem to be independent pulsation modes between 634 and 2740 µHz, and we performed preliminary asteroseismic investigations of the star utilizing six of these periods. We also identified three new light variables on the fields of white dwarf candidates: an eclipsing binary, a candidate delta Scuti/beta Cephei and a candidate W UMa-type star.

Key words: techniques: photometric – stars: individual: WD 1310+583, EGGR 120 – stars: interiors – stars: oscillations – white dwarfs.

1 INTRODUCTION

The main goal of the *TESS* (*Transiting Exoplanet Survey Satellite*; Ricker et al. 2015) all-sky survey space project, as part of NASA's Explorer programme, is to detect exoplanets at nearby and bright (up to about 15 magnitude) stars, applying the transit method. The telescope is planned to obtain data during a two-year time span, utilizing four CCD cameras, which provide a 24×96 degree field-of-view altogether. It will allow data acquisition with time samplings of 2 min for selected targets, with the possibility for 20 s sampling after commissioning. The shorter sampling times make the project feasible to obtain data for investigations into the light variations of short-period pulsating white dwarf (WD) and subdwarf stars, too.

In the framework of this ground-based photometric survey presented, we selected for observations white dwarf pulsator candidates listed by the *TESS* Compact Pulsators Working Group (WG#8), which do not lie far from the ZZ Ceti or V777 Her instability domains. We note that a more extensive search has been presented by Raddi et al. (2017), where they have compiled an all-sky catalogue of ultraviolet, optical and infrared photometry, and presented data for almost 2000 bright white dwarfs and six ZZ Ceti candidates.

ZZ Ceti (or DAV) stars are short-period and low-amplitude pulsators with 10 500–13 000 K effective temperatures, while their hotter siblings, the V777 Her (or DBV) stars, can be found at effective temperatures of roughly 22 000–31 000 K. Both show light variations caused by non-radial *g*-mode pulsations with periods between ∼100–1500 s, typically with ∼mmag amplitudes. For reviews of the theoretical and observational aspects of pulsating white dwarf studies, see the papers of Fontaine & Brassard (2008), Winget & Kepler (2008), Althaus et al. (2010), and the recent review on ZZ Ceti pulsations based on *Kepler* observations of Hermes et al. (2017). We also refer to the theoretical work of Van Grootel et al. (2013), concerning the reconstruction of the boundaries of the empirical ZZ Ceti instability strip up to the domain of the extremely low-mass DA pulsators. In addition, we also mention the observations of the so-called 'outburst' events, which means recurring increases in the stellar flux in DAV stars being close to the red edge of the instability strip (see e.g. Bell et al. 2017).

2 OBSERVATIONS AND DATA ANALYSIS

We performed the observations with the 1-m Ritchey–Chrétien–Coudé telescope located at the Piszkéstető mountain station of Konkoly Observatory, Hungary. We obtained data with an Andor iXon+888 EMCDD and an FLI Proline 16803 CCD camera in white

light. The exposure times were between 5 and 40 s, depending on the weather conditions and the brightness of the target.

Raw data frames were treated the standard way utilizing IRAF[1] tasks: they were bias, dark and flat corrected before the performance of aperture photometry of field stars and low-order polynomial fitting to the resulting light curves, correcting for low-frequency atmospheric and instrumental effects. This latter smoothing of the light curves did not affect the known frequency domain of pulsating DA and DB stars. The comparison stars for the differential photometry were checked for variability or any kind of instrumental effects. Then, we converted the observational times of every data point to barycentric Julian dates in barycentric dynamical time (BJD$_{TDB}$) using the applet of Eastman, Siverd & Gaudi (2010).[2]

We analysed the daily measurements with the command-line light-curve fitting program LCFIT (Sódor 2012). LCFIT has linear (amplitudes and phases) and nonlinear (amplitudes, phases and frequencies) least-squares fitting options, utilizing an implementation of the Levenberg–Marquardt least-squares fitting algorithm. The program can handle unequally spaced and gapped datasets and is easily scriptable.

We performed standard Fourier analyses of the whole dataset on WD 1310+583 with the photometry modules of the Frequency Analysis and Mode Identification for Asteroseismology (FAMIAS) software package (Zima 2008). Remaining traditional (see Breger et al. 1993), we accepted a frequency peak as significant if its amplitude reached a signal-to-noise ratio (S/N) of 4.

2.1 Target selection strategy

Our list of targets selected for observations is primarily based on the list of DAV and DBV candidate variables collected by the *TESS* Compact Pulsators Working Group No. 8 (WG#8) proposed for 20 s cadence observations. This list of targets was compiled from the Monteral White Dwarf Database (MWDD),[3] which is a collection of white dwarf stars with their physical parameters, in many cases originating from different authors. Thus, it presents an overall view of a queried target, including its atmospheric parameters, coordinates and brightness values in different bandpasses, and an optical spectrum. For a more detailed description of the MWDD, we refer readers to the paper of Dufour et al. (2017).

We chose variable candidates close to the DAV or DBV empirical instability strips considering their effective temperature (T_{eff}) and surface gravity (log g), and altogether 14 white dwarf variable candidates were observed in the 2017 March–November term.

3 STARS SHOWING NO LIGHT VARIATIONS

12 out of the 14 stars in our sample were not observed to vary (NOV stars). We list the log of their observations in Table 1. We did not find any significant frequencies in their Fourier transform (FT) that would suggest that pulsation operates in them.

The significance levels for the different light curves were calculated by computing moving averages of the FTs of the measurements, which provided us with an average amplitude level ($\langle A \rangle$). If a target was observed on more than one night, we utilized the

FT of all the available data. We considered a peak significant if it reached or exceeded the $4\langle A \rangle$ level. Table 1 also summarizes these $4\langle A \rangle$ significance levels in mmag in parentheses; they were found to be around 1–2 mmag in most cases.

We present representative light curves of these NOV stars and the FTs of the observations in Fig. 1 and in Appendix A1, respectively.

4 NEW VARIABLES

We successfully identified two new DA white dwarf variables (EGGR 120 and WD 1310+583) in our sample, and three new light variables of other types amongst the field stars: a candidate delta Scuti/beta Cephei, a candidate W UMa-type star and an eclipsing binary.

Table 2 shows the journal of observations of the new WD light variables.

4.1 EGGR 120

EGGR 120 ($V = 14.8$ mag, $\alpha_{2000} = 16^h39^m28^s$, $\delta_{2000} = +33^d25^m22^s$) was found to be a light variable by one night of observation.

Fig. 2 shows its light curve and the corresponding FT. We detected only one significant frequency at 1332 µHz with 2.3 mmag amplitude. This frequency value corresponds to ∼751 s periodicity, which places this star in the class of cool DAV stars (Mukadam et al. 2006), in agreement with its low estimated effective temperature. We plan to observe the star during the next observing season to obtain a more complete picture of its pulsation properties.

4.2 WD 1310+583

WD 1310+583 ($B = 13.9$ mag, $\alpha_{2000} = 13^h12^m58^s$, $\delta_{2000} = +58^d05^m11^s$) was observed on eight nights during the 2017 March–July term. We performed most of the measurements in July, when during a one-week observing session six out of the seven nights were clear.

Fig. 3 and Appendix B1 shows the light curves of the observations and their FTs, respectively.

Considering the FTs, it is conspicuous that the amplitudes of frequencies vary from night to night. This might indicate real amplitude variations; that is, the energy content of some frequencies may vary in short time scales. Amplitude and phase variations are well-known phenomena amongst pulsating white dwarf stars, observed both from the ground (see e.g. the short overview of Handler 2003) and from space (e.g. GD 1212, Hermes et al. 2014). However, we have to be cautious in the interpretation of these phenomena as true changes in the amplitudes and phases, as the beating of closely spaced frequencies could also be a possible explanation.

The Fourier analysis of the whole dataset resulted in the determination of 17 frequencies, which are listed in Table 3.

Considering the frequencies in Table 3, we determined closely spaced peaks with frequency separations of 0.08, 4.6 and 4.7 µHz. There are at least two possibilities: these are the results of short-term amplitude variations, or, in the case of the similar 4.6 and 4.7 µHz separations, rotationally split frequencies can be found at these domains.

There are also more widely spaced doublets, which could also originate from rotational splitting of frequencies. Their separations are 25.8, 27.6 and 29.8 µHz, that is, close to each other. Assuming that these are rotationally split $l = 1$ frequencies ($m = 0$, 1 or $m = -1$, 0 pairs), the star's rotational period may be around 5 h,

---

[1] IRAF is distributed by the National Optical Astronomy Observatories, which are operated by the Association of Universities for Research in Astronomy, Inc., under cooperative agreement with the National Science Foundation.
[2] http://astroutils.astronomy.ohio-state.edu/time/utc2bjd.html
[3] http://dev.montrealwhitedwarfdatabase.org/home.html

Table 1. Summary of our observations of NOV stars performed at Piszkéstetői mountain station. 'Exp' is the integration time used, N is the number of data points and δT is the length of the dataset including gaps. In the comment column, we list the $4\langle A \rangle$ significance levels in mmag in parentheses.

Run	UT date (2017)	Start time (BJD-2 45 0000)	Exp. (s)	N	δT (h)	Comment
EGGR 116:						NOV(1)
01	Mar 21	7834.377	30	1505	6.70	
02	Mar 30	7843.371	10	2350	6.54	
EGGR 162:						NOV(1)
01	Sep 15	8012.298	10	807	2.97	
EGGR 311:						NOV(2)
01	Nov 14	8072.259	30	679	6.28	
02	Nov 22	8080.188	30	384	3.55	
GD 190:						NOV(4)
01	Apr 25	7869.336	30	409	4.07	
GD 426:						NOV(2)
01	Oct 20	8047.431	30	591	5.44	
GD 83:						NOV(2)
01	Nov 22	8080.339	30	964	8.81	
HG 8-7:						NOV(2)
01	Oct 21	8048.480	15	588	3.32	
PG 1026+024:						NOV(3)
01	Mar. 16	7829.324	10	1078	4.26	
WD 0129+458:						NOV(1)
01	Oct 19	8046.221	30	1131	10.84	
02	Oct 31	8058.353	15	502	5.52	
03	Nov 15	8073.184	30	1209	11.07	
WD 0145+234:						NOV(2)
01	Oct 20	8047.219	30	533	4.94	
WD 0449+252:						NOV(2)
01	Oct 29	8056.401	40	294	3.72	
02	Oct 30	8057.321	30	827	8.79	
WD 0454+620:						NOV(1)
01	Nov 15	8072.529	10	1108	4.02	

applying the equation as follows:

$$\delta f_{k,\ell,m} = \delta m(1 - C_{k,\ell})\Omega, \qquad (1)$$

where the coefficient $C_{k,\ell} \approx 1/\ell(\ell + 1)$ for high-overtone ($k \gg \ell$) g-modes and Ω is the (uniform) rotation frequency.

Considering the 4.6 and 4.7 μHz separations, the star's rotational period could be 1.3 d. As both rotational period values are acceptable for a white dwarf (see e.g. Fontaine & Brassard 2008 or Hermes et al. 2017), we cannot decide yet which frequency separations we should consider as results of rotational splitting, if any. We also note that the daily ($1\,d^{-1} = 11.6$ μHz) alias problem also makes the determination of independent pulsation modes difficult.

In the case of the peaks around 1060 μHz, we found many closely spaced frequencies in the FT of the whole dataset. Thus, we fitted the peaks with a Gaussian and decided to list the resulting maximum frequency and the function's standard deviation at f_2 in Table 3.

Finally, the frequencies that we regard as independent modes are the following seven frequencies out of the 17 determined: f_1, f_2, f_4, f_5, f_6, f_7 and f_{12}. We mark them in the Fourier transform of the whole dataset in Fig. 4. Considering the large uncertainty in the frequency determination of f_2, we did not use it as an input for

asteroseismic investigations, but performed asteroseismic fits with the six remaining modes.

4.2.1 Preliminary asteroseimology

We built a model grid for the preliminary asteroseismic investigations of WD 1310+583 utilizing the White Dwarf Evolution Code (WDEC; Kutter & Savedoff 1969; Lamb 1974; Lamb & van Horn 1975; Winget 1981; Kawaler 1986; Wood 1990; Bradley 1993; Montgomery 1998; Bischoff-Kim, Montgomery & Winget 2008).

The WDEC evolves a hot polytrope model ($\sim 10^5$ K) down to the requested temperature, and provides an equilibrium thermally relaxed solution to the stellar structure equations. Then we are able to calculate the set of possible eigenmodes according to the adiabatic equations of non-radial stellar oscillations (Unno et al. 1989).

We utilized the integrated evolution/pulsation form of the WDEC code created by Metcalfe (2001) to derive the pulsation periods for the models with the given stellar parameters.

We calculated the periods of dipole ($l = 1$) and quadrupole ($l = 2$) modes for the model stars considering the limited visibility of high spherical degree (l) modes due to geometric cancellation effects. The goodness of the fit between the observed (P_i^{obs}) and calculated
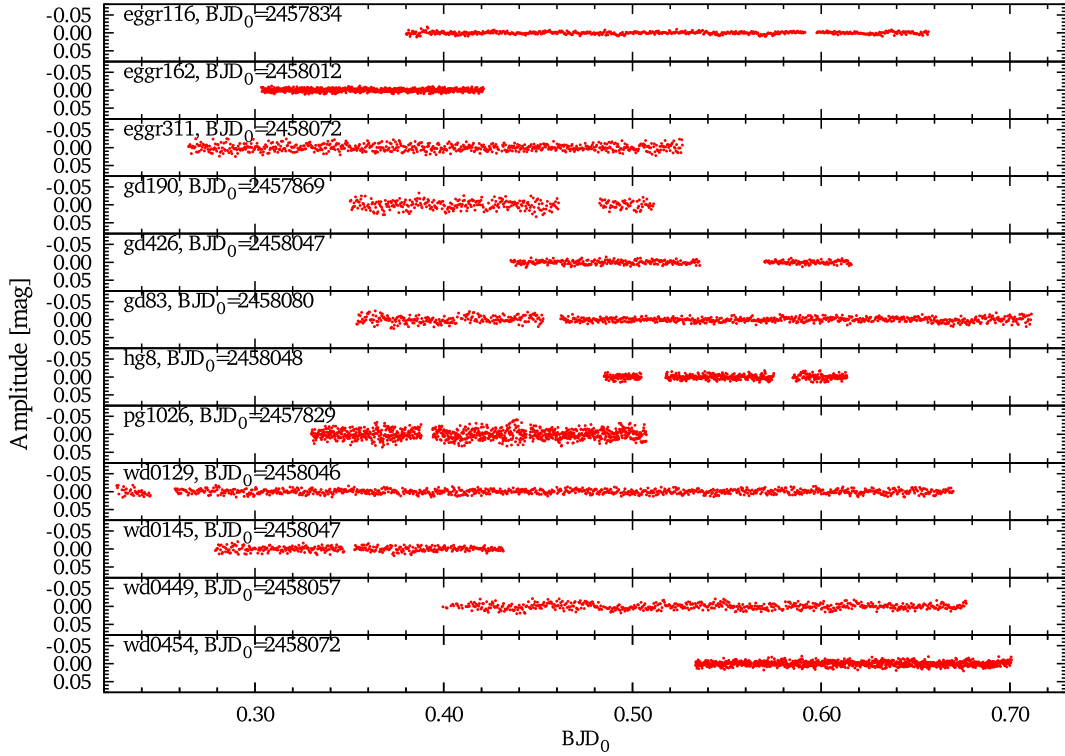
Figure 1. Representative light curves of the NOV stars.

Table 2. Summary of our observations performed at Piszkéstetői mountain station on the new light variable WD stars. 'Exp' is the integration time used, N is the number of data points and δT is the length of the datasets including gaps.

Run	UT date (2017)	Start time (BJD-2 450 000)	Exp. (s)	N	δT (h)
WD 1310+583:					
01	Mar 31	7844.296	10	2778	8.40
02	Apr 24	7868.332	10	782	3.13
03	Jul 13	7948.331	20	831	5.48
04	Jul 14	7949.405	30	388	3.61
05	Jul 16	7951.316	30	618	5.67
06	Jul 17	7952.342	20	465	2.98
07	Jul 18	7953.326	20	824	5.23
08	Jul 19	7954.314	20	705	4.53
Total:				7 391	39.02
EGGR 120:					
01	Apr 3	7847.407	10	2002	5.56

(P_i^{calc}) periods was characterized by the root mean square (σ_{rms}) value calculated for every model with the FITPER program of Kim (2007):

$$\sigma_{rms} = \sqrt{\frac{\sum_{i=1}^{N}(P_i^{calc} - P_i^{obs})^2}{N}} \qquad (2)$$

where N is the number of observed periods.

We built our model grid using the core composition profiles of Salaris et al. (1997) based on evolutionary calculations. We varied three input parameters of the WDEC: T_{eff}, M_* and M_H. The grid covers the parameter range 10 200–12 000 K in T_{eff}, 0.55–

0.85 $M_\odot$ in stellar mass, 10^{-4}–$10^{-9}\,M_*$ in M_H, and we fixed the mass of the helium layer at the theoretical maximum value of $10^{-2}\,M_*$. We used step sizes of 100 K (T_{eff}), 0.01 $M_\odot$ (M_*) and 0.2 dex (log M_H).

The mass of WD 1310+583 (log g = 8.17 by optical spectroscopy) was determined utilizing the theoretical masses calculated for DA stars by Bradley (1996), which resulted in 0.7 $M_\odot$ for the star. The error of the mass determination is about 0.03 $M_\odot$. The effective temperature of the star is derived to be 10 460 K with about 200 K uncertainty value in the optical. However, based on far-ultraviolet (FUV) spectroscopy, it turns out that WD 1310+583 may be a double degenerate binary system, in which one component with about 11 600 K effective temperature is close to the middle of the ZZ Ceti instability strip, while the other component may be much cooler, about T_{eff} = 7900 K (Gentile Fusillo et al. 2018). Furthermore, utilizing the time-tag information in the FUV spectrum, Gentile Fusillo et al. (2018) determined two pulsation frequencies of WD 1310+583 at 391 and 546 s, respectively. We did not find them in our measurements; thus these may represent new pulsation frequencies besides our findings.

We found that, utilizing our model grid, the best-fitting model (model with the lowest σ_{rms} value) has a stellar mass higher than the value determined by optical spectroscopy (0.78 $M_\odot$), but its effective temperature is close to the value calculated from the optical spectrum (10 400 K). However, note that in this case the dominant mode is $l = 2$. Assuming that at least four of the modes are $l = 1$ (including the dominant frequency), considering the better visibility of $l = 1$ modes over $l = 2$ ones, the best-fitting model has T_{eff} = 11 600 K and M_* = 0.74 $M_\odot$ (σ_{rms}=1.3 s). That is, this solution has a stellar mass close to the value determined by optical spectroscopy, but its effective temperature fits better to the value calculated from the FUV fitting.
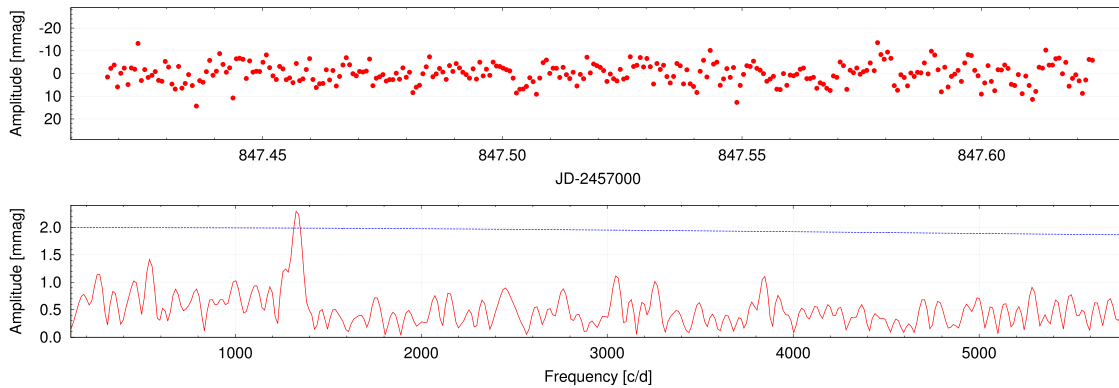
Figure 2. EGGR 120: light curve and Fourier transform. Blue line denotes the 4⟨A⟩ significance level.
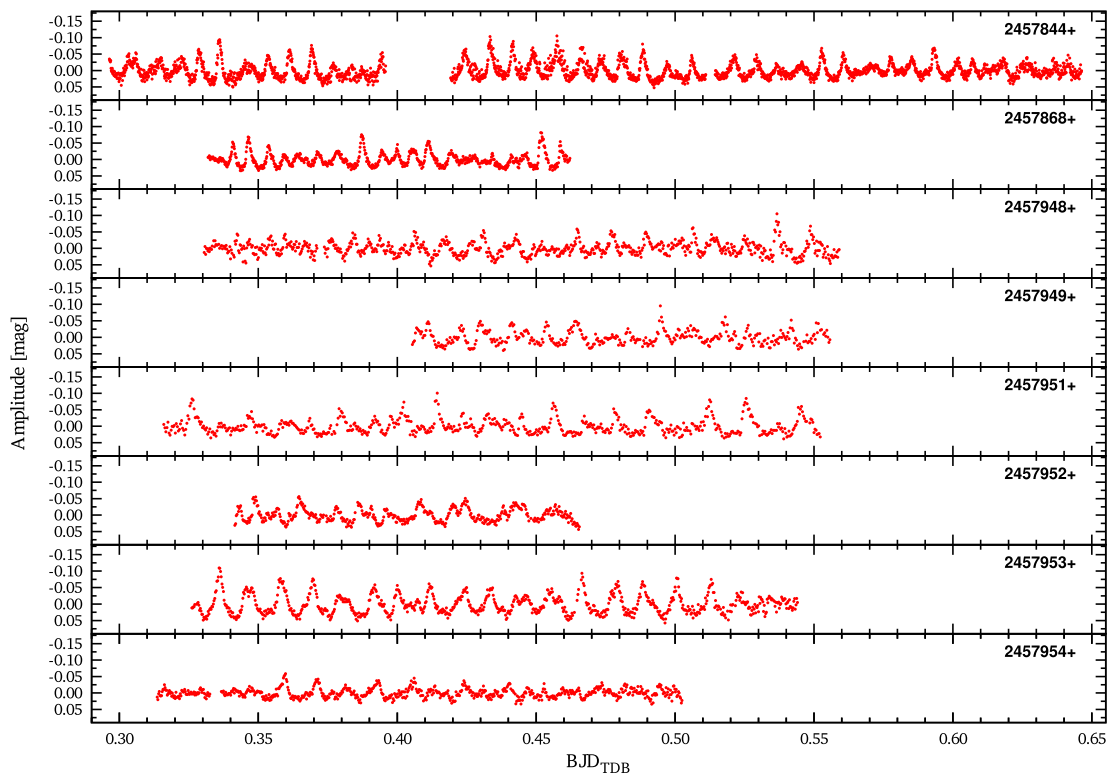

Figure 3. Normalized differential light curves of the observations of WD 1310+583.

We tried another fit adding the two frequencies found by Gentile Fusillo et al. (2018); that is, we fitted eight periods with the calculated ones. In this case, the best-fitting model has T_{eff} = 11 900 K and $M_* = 0.80\,M_\odot$ (σ_{rms}=1.6 s). This is also the best-fitting model assuming that at least five of the modes are $l = 1$.

We summarize our model findings in Table 4. Considering the effective temperatures of the best-fitting models, they seem to confirm the higher value determined by FUV observations. The relatively large-amplitude pulsations also support the idea that the pulsating component of the WD 1310+583 system may be closer to the middle of the ZZ Ceti instability strip than it is at the red edge (cf. Hermes et al. 2017).

4.3 New variables of other types

We identified an eclipsing binary on the field of WD 0129+458, a delta Scuti/beta Cephei candidate on the field of WD 0454+620, and a W UMa variable candidate on the field of GD 83. Their distances to the white dwarfs are ~4.4, 3.2 and 1.5 arcmin; that is, they do not contaminate the large (~21 arcsec) *TESS* pixels.

4.3.1 Eclipsing binary

We could observe one eclipse only (see Fig. 5). We tried to catch another minimum during further observations, but we did not succeed. Thus, we cannot tell at this moment whether we saw a main or a

Table 3. WD 1310+583: result of the Fourier analysis of the whole dataset. The frequencies are listed in order of the pre-whitening procedure. The error value for f_2 is the standard deviation of the Gaussian fitted to the peaks found around this frequency, while in the other cases errors were derived by Monte Carlo simulations.

|	f [μHz]	δf	P [s]	Ampl. [mmag]	Phase [2π]	S/N	Comment
f_1	1439.858	0.001	694.51	12.8	0.63	16.4	
f_2	1063.102	45	940.64	–	–	–	
f_3	1451.478	0.003	688.95	8.1	0.87	10.5	$\sim f_1+1\,\mathrm{d}^{-1}$
f_4	1958.452	0.001	510.61	6.9	0.16	9.8	
f_5	1751.226	0.009	571.03	6.3	0.79	8.8	
f_6	2739.544	0.002	365.02	6.3	0.79	10.2	
f_7	963.032	0.003	1038.39	7.0	0.86	9.9	
f_8	967.347	0.004	1033.76	5.9	0.27	8.1	close to f_7
f_9	1751.155	0.010	571.05	5.4	0.88	7.6	close to f_5
f_{10}	1469.611	0.003	680.45	3.6	0.69	4.6	close to f_1
f_{11}	1037.324	0.002	964.02	5.0	0.72	5.7	close to f_2
f_{12}	633.984	0.005	1577.33	6.6	0.11	8.1	
f_{13}	632.088	0.006	1582.06	5.6	0.83	6.8	close to f_{12}
f_{14}	2767.140	0.003	361.38	3.0	0.91	4.8	close to f_6
f_{15}	2890.388	0.003	345.97	2.6	0.17	4.7	$2f_1+1\,\mathrm{d}^{-1}$
f_{16}	3197.877	0.004	312.71	2.3	0.22	4.3	$\sim f_1 + f_5$
f_{17}	4493.635	0.005	222.54	1.6	0.97	4.4	$\sim f_5 + f_6$
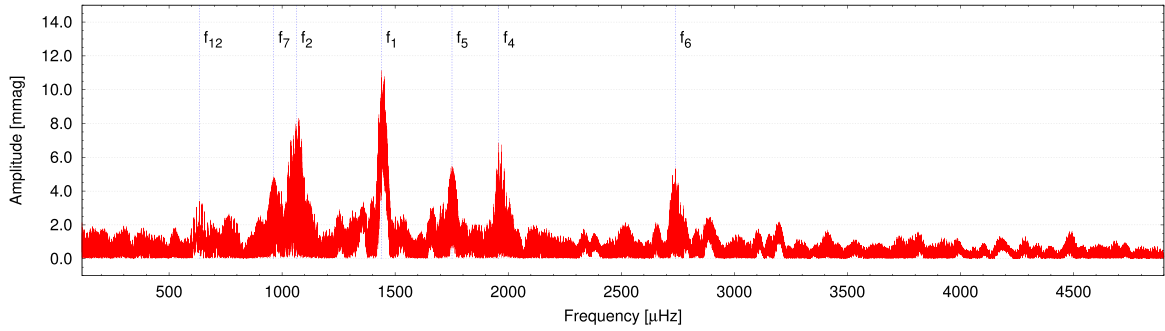
Figure 4. Fourier transform of the whole dataset obtained on WD 1310+583. We have marked the frequencies that can be regarded as independent pulsation modes with blue dashed lines (cf. Table 3).

Table 4. Best-fitting models for WD 1310+583 derived by seven periods (first two rows) and nine periods (third row).

T_{eff} (K)	$M_*/M_\odot$	-log M_{H}	Periods in seconds (l)								σ_{rms}
10 400	0.78	8.2	364.9(1)	510.6(2)	569.9(1)	694.2(2)	1038.7(2)	1579.8(1)			1.1
11 600	0.74	4.0	364.5(1)	508.9(2)	568.9(1)	694.5(1)	1037.1(2)	1576.2(1)			1.3
11 900	0.80	7.6	362.1(1)	511.3(1)	572.2(2)	692.3(1)	1038.2(1)	1575.7(1)	389.9(2)	545.7(2)	1.6
Observations:			365.0	510.6	571.0	694.5	1038.4	1577.3	390.9	545.5	

secondary minimum in our light curve. The star's 2MASS identifier is 01323981+4600441 ($J = 12.4$ mag, $\alpha_{2000} = 01^{\mathrm{h}}32^{\mathrm{m}}40^{\mathrm{s}}$, $\delta_{2000} = +46^{\mathrm{d}}00^{\mathrm{m}}44^{\mathrm{s}}$; Cutri et al. 2003).

4.3.2 *Delta Scuti/beta Cephei variable candidate*

We found one significant frequency of the light variation of this star at $15.7\,\mathrm{d}^{-1}$ ($\sim 1.5\,\mathrm{h}$) with 13 mmag amplitude (Fig. 6). This pulsational behaviour could be typical both for delta Scuti and beta Cephei stars, respectively. Colour or spectroscopical measurements could help to decide which type of pulsating variables this object belongs to; however, none of them are available at this moment. Its 2MASS identifier is 04584888+6212098 ($J = 12.0$ mag, $\alpha_{2000} = 04^{\mathrm{h}}58^{\mathrm{m}}49^{\mathrm{s}}$, $\delta_{2000} = +62^{\mathrm{d}}12^{\mathrm{m}}10^{\mathrm{s}}$).

4.3.3 *W UMa variable candidate*

A further finding is a W UMa-type variable candidate. Fig. 7 shows its light curve and Fourier spectrum. The dominant periodicity is at $6.75\,\mathrm{d}^{-1}$ ($\sim 0.15\,\mathrm{d}$). The star's 2MASS identifier is 07131730+2135152 ($J = 14.5$ mag, $\alpha_{2000} = 07^{\mathrm{h}}13^{\mathrm{m}}17^{\mathrm{s}}$, $\delta_{2000} = +21^{\mathrm{d}}35^{\mathrm{m}}15^{\mathrm{s}}$).

5 SUMMARY AND CONCLUSIONS

We aimed to perform survey observations to find new white dwarf pulsators for the *TESS* mission. For this purpose, we collected photometric time-series data on 14 white dwarf variable candidates at Konkoly Observatory during the 2017 March–November term. Besides the visual inspection of the light curves, we performed Fourier

Table 5. Physical parameters of the 14 targets observed in our survey. We denote by *G* at the surface gravity when the source of the original physical parameters is the database of Gianninas, Bergeron & Ruiz (2011). We corrected these T_{eff} and log *g* values according to the findings of Tremblay et al. (2013) based on radiation-hydrodynamics three-dimensional simulations of convective DA stellar atmospheres. In the other cases the source of the parameters was either Limoges, Bergeron & Lépine (2015) (*L*) or Bergeron et al. (2011) (*B*), respectively.

ID	Spectral type	T_{eff} (K)	log *g* (dex)	*TESS* mag.
EGGR 116	DA	13 100	7.87^G	13.6(*I*)
EGGR 162	DA	13 100	8.02^G	13.2
EGGR 311	DA	12 800	7.98^G	14.5
GD 190	DB	22 630	8.04^B	14.9(*I*)
GD 426	DA	10 920	8.10^G	15.6
GD 83	DA	10 390	7.93^G	14.9(*I*)
HG 8-7	DA	12 690	8.05^G	13.6(*I*)
PG 1026+024	DA	13 110	8.06^G	14.1(*V*)
WD 0129+458	DA	10 680	7.97^L	14.3(*I*)
WD 0145+234	DA	13 000	8.13^G	14.2
WD 0449+252	DAH	11 500	8.00^L	14.9(*V*)
WD 0454+620	DA+dM	10 960	8.88^L	12.3
EGGR 120	DA	10 170	8.03^G	14.8
WD 1310+583	DA or DA+DA	10 460	8.17^G	13.8
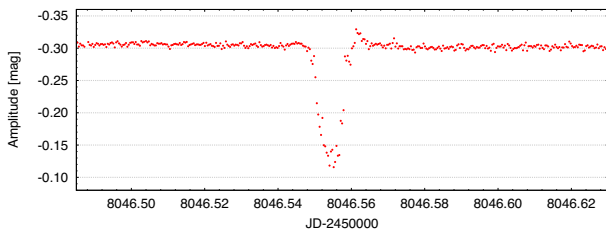
Figure 5. Light curve of the eclipsing binary found on the field of WD 0129+458.
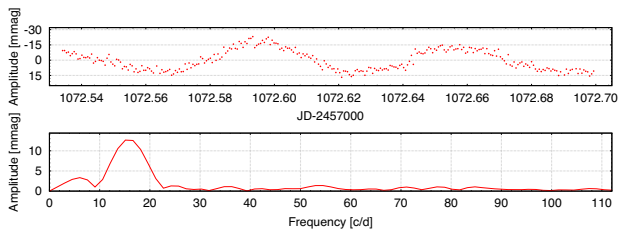
Figure 6. Light curve and Fourier transform of the variable found on the field of WD 0454+620.
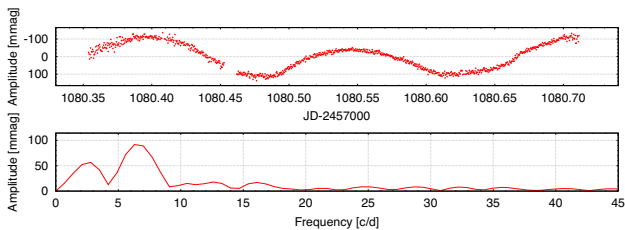

Figure 7. Light curve and Fourier transform of the WUMa-type variable candidate found on the field of GD 83.

analysis of all datasets and successfully identified two new ZZ Ceti stars: EGGR 120 and WD 1310+583. In the case of EGGR 120, which was observed on one night only, we found one significant frequency at 1332 μHz with 2.3 mmag amplitude. We could observe WD 1310+583 on eight nights altogether, and determined 17 significant frequencies in the whole dataset. Seven of them seem to be independent pulsation modes with frequencies between 634 and 2740 μHz, and we performed preliminary asteroseismic investigations of the star utilizing six of these periods.

We also identified three new variables on the fields of white dwarf candidates: an eclipsing binary, a delta Scuti/beta Cephei candidate and a W UMa-type star. The periods of their light variations are long enough that the 30 min time sampling of the full-frame images (FFIs) of *TESS* will be enough to study their pulsations and eclipses.

Fig. 8 shows the classical ZZ Ceti instability strip with plots of the known DAV stars (red filled dots) and the stars presented in this paper (green and blue dots with error bars, respectively). We collected the atmospheric parameters of known DAV stars utilizing the database of Bognár & Sódor (2016), in which the authors listed corrected T_{eff} and log *g* values for the three-dimensional dependence of convection for most of the objects. In Table 5 we summarize the physical parameters of the 14 targets observed in our survey.

The newly discovered relatively bright WD variables are excellent targets for small telescopes, especially WD 1310+583, which shows larger-amplitude light variations than EGGR 120. Considering Fig. 8, they lie close to the middle and the red edge of the ZZ Ceti instability domain, respectively, with good agreement with their pulsational properties: relatively long periods and non-sinusoidal light curves, and, in the case of the longer observed WD 1310+583, the closely spaced frequencies suggest the presence of amplitude and phase variations. With space photometry and additional ground-based follow-up observations planned, hopefully we will learn much more about their pulsation behaviour in the near future.

Considering all the proposed white dwarf targets for *TESS* observations, almost all of them have only been observed from the ground up to now. Sometimes these observations are even limited to the usually short discovery light curves. The 27 d or longer, uninterrupted *TESS* measurements will outperform most of the available data on these bright pulsators. Data simulations also show, that in terms of signal-to-noise ratio, considering equal monitoring time, *TESS* data are expected to be roughly equivalent to *Kepler* data obtained for stars five magnitudes fainter. Besides, taking into account that pulsating white dwarfs down to magnitude 19 have been successfully observed with *K2*, this suggests that *TESS* can provide useful data at least down to magnitude ∼15.
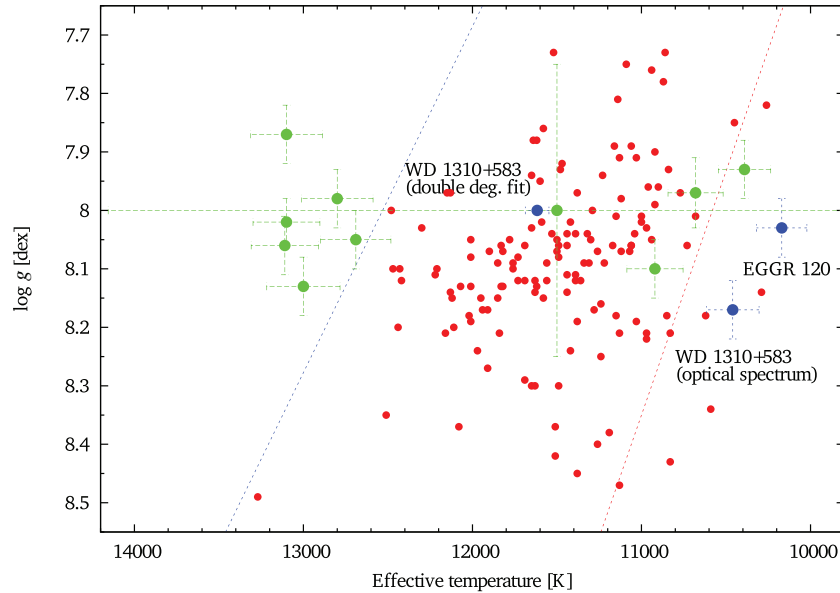
Figure 8. Known variable stars (red filled dots) and the newly observed ZZ Ceti candidates and DAVs (green and blue dots, respectively) in the T_{eff}–$\log g$ diagram. Blue and red dashed lines denote the hot and cool boundaries of the instability strip, according to Tremblay et al. (2015). In the case of WD 1310+583, the double degenerate solution assumes two white dwarfs with fixed $\log g = 8.0$ dex values. The effective temperature was determined by the simultaneous fitting of both the optical spectrum and the FUV to near-infrared photometric data with two white dwarf models (Gentile Fusillo et al. 2018).

REFERENCES

Althaus L. G., Córsico A. H., Isern J., García-Berro E., 2010, A&AR, 18, 471

Bell K. J., Hermes J. J., Montgomery M. H., Winget D. E., Gentile Fusillo N. P., Raddi R., Gänsicke B. T., 2017, in Tremblay P.-E., Gaensicke B., Marsh T., eds, ASP Conf. Ser. Vol. 509, 20th European White Dwarf Workshop. Astron. Soc. Pac., San Francisco, p. 303

Bergeron P. et al., 2011, ApJ, 737, 28

Bischoff-Kim A., Montgomery M. H., Winget D. E., 2008, ApJ, 675, 1512

Bognár Z., Sódor A., 2016, Inf. Bull. Var. Stars, 62, 6184

Bradley P. A., 1993, PhD thesis, Univ. Texas, Austin

Bradley P. A., 1996, ApJ, 468, 350

Breger M. et al., 1993, A&A, 271, 482

Cutri R. M. et al., 2003, 2MASS All Sky Catalog of Point Sources, NASA/IPAC Infrared Science Archive

Dufour P., Blouin S., Coutu S., Fortin-Archambault M., Thibeault C., Bergeron P., Fontaine G., 2017, in Tremblay P.-E., Gaensicke B., Marsh T., eds, ASP Conf. Ser. Vol. 509, 20th European White Dwarf Workshop. Astron. Soc. Pac., San Francisco, p. 3

Eastman J., Siverd R., Gaudi B. S., 2010, PASP, 122, 935

Fontaine G., Brassard P., 2008, PASP, 120, 1043

Gentile Fusillo N. P., Tremblay P.-E., Jordan S., Gänsicke B. T., Kalirai J. S., Cummings J., 2018, MNRAS, 473, 3693

Gianninas A., Bergeron P., Ruiz M. T., 2011, ApJ, 743, 138

Handler G., 2003, in Sterken C., ed., ASP Conf. Ser. Vol. 292, Interplay of Periodic, Cyclic and Stochastic Variability in Selected Areas of the H-R Diagram. Astron. Soc. Pac., San Francisco, p. 247

Hermes J. J. et al., 2014, ApJ, 789, 85

Hermes J. J. et al., 2017, ApJS, 232, 23

Kawaler S. D., 1986, PhD thesis, Univ. Texas, Austin

Kim A., 2007, PhD thesis, Univ. Texas, Austin

Kutter G. S., Savedoff M. P., 1969, ApJ, 156, 1021

Lamb D. Q., Jr, 1974, PhD thesis, Univ. Rochester

Lamb D. Q., van Horn H. M., 1975, ApJ, 200, 306

Limoges M.-M., Bergeron P., Lépine S., 2015, ApJS, 219, 19

Metcalfe T. S., 2001, PhD thesis, Univ. Texas, Austin

Montgomery M. H., 1998, PhD thesis, Univ. Texas, Austin

Mukadam A. S., Montgomery M. H., Winget D. E., Kepler S. O., Clemens J. C., 2006, ApJ, 640, 956

Raddi R. et al., 2017, MNRAS, 472, 4173

Ricker G. R. et al., 2015, J. Astron. Telesc. Instrum. Syst., 1, 014003

Salaris M., Domínguez I., García-Berro E., Hernanz M., Isern J., Mochkovitch R., 1997, ApJ, 486, 413

Sódor Á., 2012, Konkoly Observatory Occasional Technical Notes, Konkoly Observatory Budapest, Hungary, 15

Tremblay P.-E., Ludwig H.-G., Steffen M., Freytag B., 2013, A&A, 559, A104

Tremblay P.-E., Gianninas A., Kilic M., Ludwig H.-G., Steffen M., Freytag B., Hermes J. J., 2015, ApJ, 809, 148

Unno W., Osaki Y., Ando H., Saio H., Shibahashi H., 1989, Nonradial oscillations of stars, University of Tokyo Press, Tokyo

Van Grootel V., Fontaine G., Brassard P., Dupret M.-A., 2013, ApJ, 762, 57

Winget D. E., 1981, PhD thesis, Univ. Rochester

Winget D. E., Kepler S. O., 2008, ARA&A, 46, 157

Wood M. A., 1990, PhD thesis, Univ. Texas, Austin

Zima W., 2008, Communications in Asteroseismology, 155, 17

APPENDIX A:

Fig. A1 shows Fourier transforms of the light curves of NOV stars. Blue lines denote the 4⟨A⟩ significance level for the detection of possible pulsation frequencies.

Figure A1. Fourier transforms of the light curves of NOV stars. Blue lines denote the 4⟨A⟩ significance level for the detection of possible pulsation frequencies.
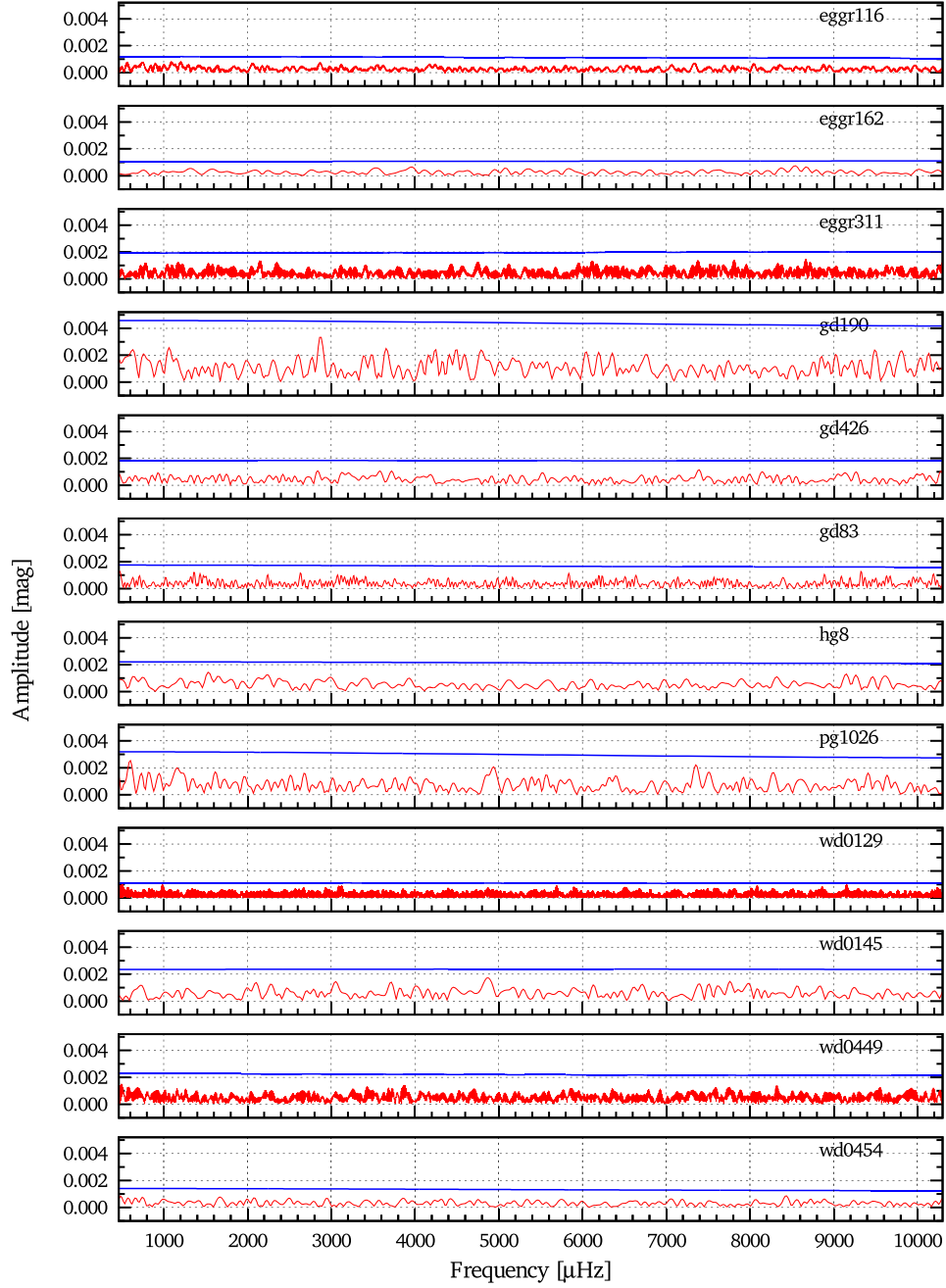
APPENDIX B:

Fig. B1 shows Fourier transforms of the nightly observations of WD 1310+583. Blue lines denote the $4\langle A \rangle$ significance levels.
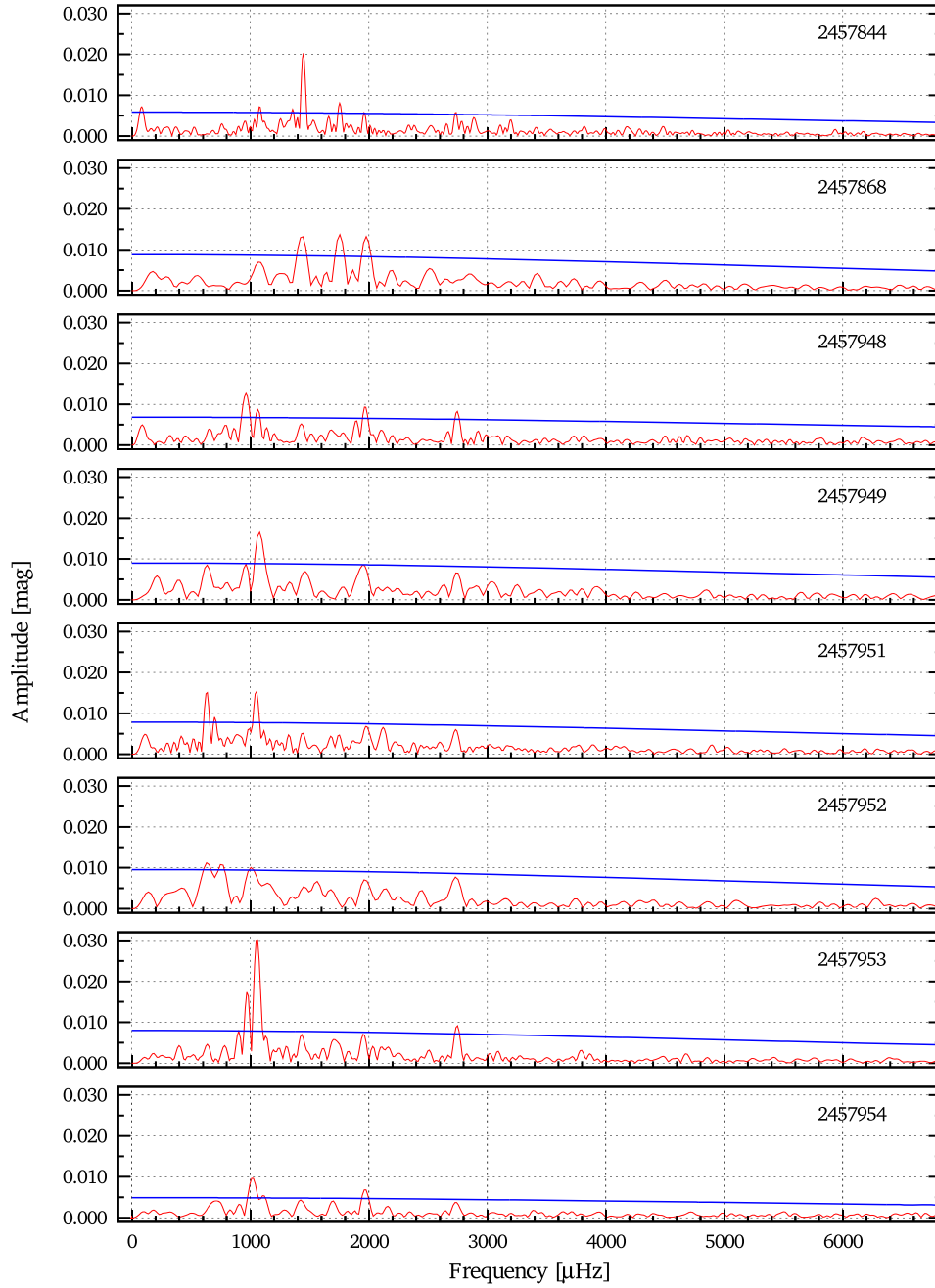

Figure B1. Fourier transforms of the nightly observations of WD 1310+583.

This paper has been typeset from a T_EX/L^AT_EX file prepared by the author.